Laser and Particle Beams (1997), *vol.* 15, *no.* 4, *pp.* 485–493
Printed in the United States of America

Determination of the color temperature in laser-produced shocks

By SIMONE BOSSI,* TOM A. HALL,*
MOHAMMED MAHDIEH,* DIMITRI BATANI,**
MICHEL KOENIG,† JOTHY KRISHNAN,†
ALESSANDRA BENUZZI,† JEAN MICHEL BOUDENNE,†
AND THORSTEN LÖWER‡
*University of Essex, Dept. of Physics, Wivenhoe Park, 504 3SQ Colchester, United Kingdom
**University of Milan, Dept. of Physics, via Celoria 16, 20133 Milan, Italy
†LULI, Ecole Polytechnique, 91128 Palaiseau, France
‡Max-Planck-Institut fur Quantenoptik, Garching, Munich, Germany

(Received 16 October 1996; Accepted 8 June 1997)

Experimental results on the determination of the color temperature in shock waves produced with lasers are presented. The method is based on imaging the target rear side in two different spectral windows and on using phased zone plates to produce high-quality shocks. The shock velocity is also measured, allowing, with the use of the equation of state, the real shock temperature to be deduced and compared with the measured color temperature.

1. Introduction

The study of strongly compressed materials and in particular the knowledge of their equations of state (EOS) is an important research field of interest in astrophysics (Ross & Nellis 1982), and for inertial confinement fusion (ICF) (Nuckolls *et al.* 1972). At high pressures, that is, above one Megabar, only a few experimental data are available. Hence, various theoretical models have to be used to interpolate and extrapolate them in a wide range of pressures, without being able to discriminate among the different predictions of such models.

This lack of experimental data is due to the fact that, until recently, the only way to compress materials to pressures in the multi-Megabar domain was to use dynamic shocks generated through nuclear explosions (Ragan *et al.* 1982). Nowadays, a valid alternative is represented by the use of high-power lasers. Recently it has been demonstrated that extremely high pressure (0.75 Gbar) can be produced with lasers and the use of flyer plates (Cauble *et al.* 1993). Also, the generation of high-quality shocks needed for EOS experiments has been demonstrated with direct drive (Batani *et al.* 1996) and indirect drive (Löwer *et al.* 1994).

EOS measurement for a given material can be performed when two shock parameters are experimentally measured in the same laser shot, making use of Hugoniot–Rankine relations (Zeldovich & Raizer 1966), which regulate the propagation of planar shocks. One parameter that is easily measured is the shock velocity D. This already allows "relative" EOS measurements by using appropriate targets and a reference material with a well-known EOS (Benuzzi *et al.* 1996a). When this is not possible, an "absolute" EOS experiment must be performed, which requires measuring a second parameter, usually a much more difficult task.

Such a second parameter, which may be determined is the shock temperature, that, for instance, in experiments at lower pressures (realized with conventional explosives or gas guns), is measured with fast multichannel pyrometers. This is not possible in laser experiments due to

 0263-0346/97 $11.00 + .10

the high temporal resolution that is needed, which usually implies the use of streak cameras as detectors. Some preliminary attempts in this direction have been made by Ng *et al.* (1985a, 1985b), who have recorded the spectrum emitted in the visible region by the target rear side with a streak camera coupled to a prism and interpolated their results with a blackbody curve. They have also tried to determine such temperature by measuring the total power emitted by the target rear side with an absolute calibration of their streak camera. Even if their results were quite encouraging, some problems remain to be addressed. First, the two methods do not actually measure the same parameter (the first one measures the "spectral" temperature, while the second the "brightness" temperature). Second, the time resolution in the experiments was not too high (of the order of 100 ps). Third, for the temperatures obtained in their experiments (1–4 eV typically), the maximum of blackbody emission lies in the VUV or XUV region, which makes interpolation of a blackbody tail in the visible region not so sensitive to actual variations of emission temperature.

Also, in such experiments, it is quite difficult to obtain high-quality shocks, that is, planar and hence with uniform parameters, and, above all, to check them shot by shot. Finally, the "real" shock temperature is not measured independently so that it is difficult to assess the reliability of the method. In this paper, we present some preliminary results of an experiment and a method to measure the color temperature of the target rear side, which is based on:

1. the direct-drive approach coupled with the phased zone plates (PZPs) optical smoothing technique to obtain a flat top intensity profile in the focal spot (Koenig *et al.* 1994). Planar shock fronts are then produced, allowing precise measurements of shock parameters; and
2. the use of an imaging technique by which we record the target rear-side emission in two different spectral regions as a function of time and space on the same detector (an optical streak camera). Imaging allows the shock quality to be checked on each laser shot and also the use of stepped targets. Hence, the shock velocity can be determined on the same laser shots and, if a material with a well-known EOS is used, the shock temperature can be deduced by using Hugoniot–Rankine relations.

Hence, it must be clearly stated that the objective of the experiment is not to measure the shock temperature (through rear-side emissivity) and the shock velocity independently to perform absolute EOS measurements, but rather to use materials with a well-known EOS to assess the reliability of the proposed method, and to compare the measured value of the color temperature with the deduced shock temperature to study the possible causes that introduce a difference between the two. For this we used aluminum targets, which have a well-known EOS in the investigated range of pressures ($\leq$10 Mbars).

Also, in this paper we mainly present the experimental setup and some preliminary results. A detailed presentation, with a deeper discussion of all of our results, will be presented in a following paper.

2. Principle of the experiment

The aim of the experiment is to measure the electromagnetic emission of the target rear side in two distinct spectral bands (in the visible region). The shock velocity D is also measured at the same time.

The principle of the experiment is shown in figure 1. The shock wave is generated by focusing an intense laser beam on a single-step Al target. The use of such targets allows a direct and precise determination of the shock velocity shot by shot (Koenig *et al.* 1994). Indeed, D can be obtained by measuring the shock breakthrough times from the base and the step. When the shock arrives on the target rear surface, there is an increase of the electromagnetic (EM) emission. As it is well known, the material behind the shock front is in thermal equilibrium and

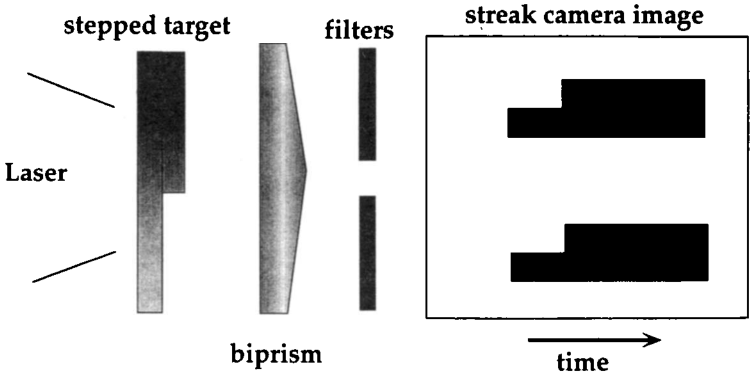

FIGURE 1. Principle of the experiment.

hence radiates according to Kirchoff's law [see, e.g., Landsberg (1976) or Smirnov (1977)], that is,

$$I(\nu,T)/A(\nu,T) = I_b(\nu,T), \tag{1}$$

where $I(\nu,T)$ is the luminous flux emitted in the spectral interval $d\nu$, $I_b(\nu,T)$ is the blackbody spectrum [both $I_b(\nu,T)$ and I_b are measured in the same units, for example, W/m^2s^{-1})]

$$I_b(\nu,T) = \frac{2\pi h\nu^3}{c^2}\frac{1}{e^{h\nu/kT} - 1}, \tag{2}$$

and $A(\nu,T)$ is the absorbing power of the body (i.e., the ratio between the incident and the re-emitted power). Hence, in general, $A(\nu,T) \leq 1$, while it is always $= 1$ for a blackbody by definition. For a plasma layer such absorption is given by

$$A(\nu,T) = \exp\left[-\int dx k_\nu(x,T)\right], \tag{3}$$

where $k_\nu(x,T)$ is the plasma opacity at the position x (characterized by a temperature T) and at the frequency ν.

Then, the total intensity emitted at a frequency ν by the expanding plasma will be given by the formula:

$$I(\nu) = \int_0^\infty dx I_b(\nu,x) k\nu(x) \exp\left[-\int_0^x dx' k\nu(x')\right]. \tag{4}$$

Here, the second exponential term corresponds to the attenuation of the light emitted at the position x in the plasma before it actually reaches the observer (the detector) and it can be written as $\exp(-\tau)$, where τ is the plasma optical density. Hence, the second integral is extended over the interval $(0,x)$, where 0 refers to the observer position, as shown in figure 2. Instead, the first term in the formula, $[dxI_b(\nu,x)k_\nu(x)]$, corresponds to the emission of the plasma layer at position x with thickness dx (it is difficult to assess how much such emission differs from blackbody due to the lack of information about opacities in the visible region).

The first integral is formally extended over the interval $(0, \infty)$ even if, in reality, only layers with optical densities τ up to a few units need to be considered. Moreover, even if equation (4) is an integral formula, which takes into account the contributions from all of the plasma layers, in reality, during the rear face expansion (see figure 2), the emission mainly comes from a given

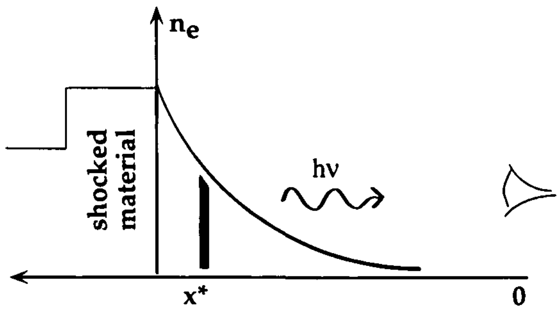

FIGURE 2. Density profile of the target rear face at shock arrival. The emission mainly comes from a layer x^*, which corresponds to an optical density $\tau \approx 1$ with respect to the observer ($x = 0$).

layer x^* of the density profile, which corresponds to an optical density $\tau \approx 1$ with respect to the observer (Fortov *et al.* 1992). Indeed, light emitted from denser layers will suffer big attenuation, while lower density and temperature layers (at smaller x) will have negligible emission.

One important exception to the validity of equation (4) is at very early times, when the plasma originating from the target rear side has not yet expanded sufficiently, and so its screening effect is also small. Hence, the total emitted power will be due to all of the layers up to the critical layer x_c (characterized by the critical density n_c) and beyond. Indeed, even the light emitted from plasma regions that are overcritical, but that are inside a skin depth, will be able to escape from the plasma. These important effects are discussed in deep details in Celliers and Ng (1993). Here, for the moment, we are interested mainly in a presentation of the method and a first qualitative discussion and we will not consider them.

In our experiment, the emission of the target rear surface is recorded in two spectral regions by splitting its image onto the slit of a visible streak camera. Two time–space resolved images of the shock breakthrough in two "channels" of emission are then obtained. The ratio between these two spectral intensities, at a given time, gives an equivalent temperature (called "color temperature") of the plasma at that time, where a blackbody emission is assumed.

Such a measured color temperature T^* will correspond to the layer x^* from which emission mainly comes. In particular, at shock arrival (assuming there is no preheating effect ahead of the shock front), the density profile on the rear side will be step-like. In this case, the temperature T^* will be the color temperature of the shocked and compressed rear side of the target, provided the utilized diagnostics have sufficient time resolution so that there is no temporal averaging effect. Let us note explicitly that, even in this case (again, neglecting the problems related to critical layer and skin depth effects too), the emission will be determined by Kirchoff's law and will not correspond to a blackbody emission. Hence, even in this case, T^* will not correspond to the true shock temperature T_s.

In other words, the equivalent temperature T^* is not the real plasma temperature at any time, and it is evident from formula (4) that to find the real plasma temperature, the knowledge of plasma opacities in the visible region of the EM spectrum is needed, which is, at the moment, a difficult task.

In the present experiment, we are able to get the "real" shock temperature T_s by measuring the shock velocity D and using available EOS data. This will allow a comparison between T_s and T^* and the study of the effects that cause them to be different. In the end, some indirect data on plasma opacities in the visible region for such high-density, low-temperature plasma might possibly be inferred.

3. Experimental setup

In figure 3, we schematically describe the experimental setup. The target was irradiated with a $\lambda = 0.53$ μm Gaussian laser pulse with a full width at half measure (FWHM) $\approx$ 600 ps. The laser pulse was focused by an $f/6$ lens ($f = 50$ cm) onto the target and a PZP was placed just after the lens to produce a flat-top profile with a FWMH $\approx$ 350 μm and a flat region of $\approx$200 μm. Spatially averaged intensities up to $3 \cdot 10^{13}$ W/cm^2 were then obtained on the target surface. An optical system made of a camera lens and a biprism allowed the image of the target rear face to be split into two onto the slit of a visible streak camera working at 100 ps/mm. Each image was then recorded by using two different colored filters. The spectral sensitivities of the two "channels" (taking into account the filters and the streak camera sensitivities) had maximum around 400 nm (blue) and 600 nm (red), as shown in figure 4a. Figure 4b shows the ratio I_r/I_b as a function of the plasma equivalent temperature calculated using such spectral sensitivities. A 512 $\times$ 512 pixel, 12-bit charge-coupled device (CCD) camera was used to record the time-resolved images. The arrival time of the driving laser pulse on the target was given by a fiducial trace recorded by the streak camera via an optical fiber.

We note in particular that:

1. to obtain the curves in figure 4a, we have measured the transmissivity of all the used optics and filters with a spectrophotometer and we have used the constructor's data for the streak camera sensitivity. We are also currently testing the sensitivity of the procedure to small changes in the curves in figure 4a and attempting a direct on-site calibration by making use of a tungsten lamp and an optical pyrometer.
2. a temporal resolution of ± 5 ps has been achieved. This has been achieved because a 50-μm slit has been used with a 100-ps/mm time scale on the streak camera and considering that the streak camera intensifier has a 1.5 magnification and a 20 lines/mm resolution. The streak camera time scale has been given by the producer but has also been calibrated on site using the LULI femtosecond laser and an arrangement of semireflecting thin glasses to produce a pulse train (Benuzzi *et al.* 1996b).
3. owing to chromatic effects, that is, to the dependence of index of refraction of glass $n(\lambda)$ from wavelength of light, an apparent time shift can arise between the signals recorded in the blue and in the red channels. In particular, the index of refraction n is slightly bigger

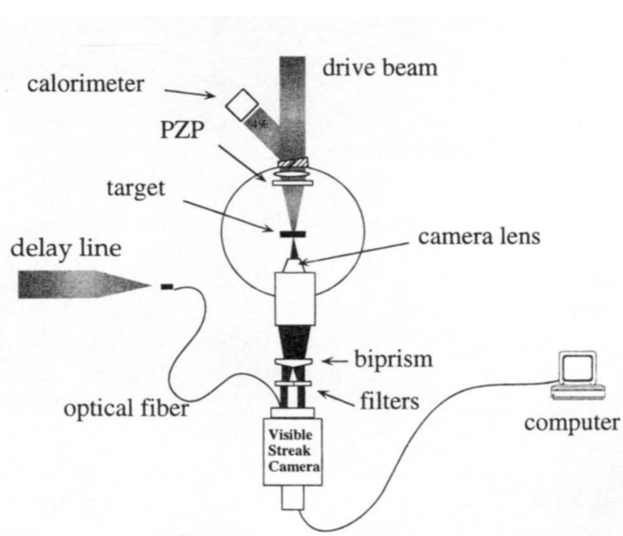

FIGURE 3. The experimental setup. The photographic objective is a camera lens (Olympus 50 mm, 1/1.2).

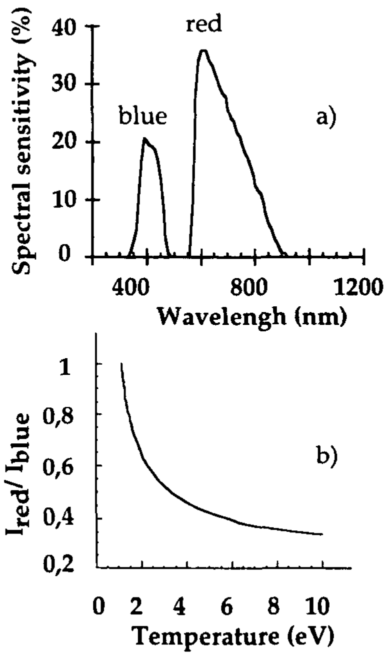

FIGURE 4. (a) Spectral sensitivity in the two channels of emission. (b) Plot of the equivalent temperature T^* as a function of the ratio I_r/I_b.

for blue and so the velocity of "blue" light in the glass is slightly smaller and the signal arrives later. This difference increases with the total thickness of glass used, that is, the camera lens, the biprism, and the interaction chamber window. We have verified that for the typical glasses used [which are characterized by $\Delta n/n \approx 1\%$, see, e.g., *Optics Guide 5*, published by Melles-Griot, or Landsberg (1976)] and total thickness ($\approx$ a few centimeters), this time delay is still of the order of our time resolution ($\approx$5 ps).

4. Results

Figure 5 shows the laser spatial intensity profile in the focal spot and the streak camera image of the produced shock obtained with a simple Al foil (used to test the flatness of the shock). The flat region in the shock front extends over 200 μm, corresponding to the laser focal spot profile. In such conditions, it is then possible to use stepped targets because the pressure is the same on both sides of the step.

Figure 6 shows an experimental result obtained with an Al target with a 9-μm base and a 4.1-μm step. Numerical simulations have shown that, in aluminum, D reaches a constant value after travelling about 8–9 μm in the target and it remains constant up to 40 μm. Thus, D is constant in a target with a 9-μm base. Measured shock velocities are of the order of 20 μm/ns (km/s), which correspond to a pressure $P_s \approx 6$ Mbar according to SESAME EOS (Holián *et al.* 1984).

Concerning the determination of T^*, figure 7 shows the emissions in the two spectral regions as a function of time. Both channels show a sharp peak of emission followed by a slow decay due to plasma expansion after shock breakout. It has been shown that such emissivity profiles indicate that there are no preheating effects due to hard X rays, which, in our case, could be produced in the plasma corona (Löwer *et al.* 1994). The equivalent temperature is plotted in

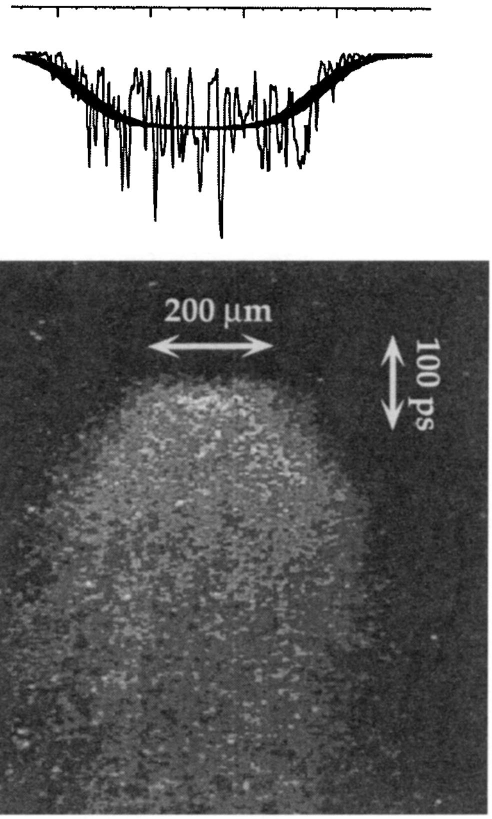

FIGURE 5. Spatial intensity profile in the focal spot (top) and the streak camera image of the produced shock obtained with a simple Al foil (bottom).

figure 8. As expected, there is a temporal correspondence between maximal temperature and the maximal emission in both channels. A maximum value $T^* \approx$ 2–2.5 eV has been measured at shock arrival while, according to SESAME tables, with our shock velocity, the expected shock temperature is T_s = 3.5 eV.

Among the possible causes for such discrepancy, we think that four should be considered in particular. First, T^* and T_s, at shock arrival, may be different due to the effect of plasma opacities, that is, the plasma could be in thermal equilibrium, but its emission, determined by Kirchoff's law, could be different from a pure blackbody. Second, the temporal resolution may be too low. Indeed, some preliminary works (Huller *et al.* 1994) have shown that the first flash of light from target rear side (corresponding to shock breakthrough) will last for only a few ps. Then our data should be coupled to a model of plasma expansion to extrapolate the value of T_s from the value of T^* at later times. Third, the effects related to the critical layer and skin depth discussed by Celliers and Ng (1993) could be important in our case, to question the validity of equation (4). Finally, it must be pointed out that the temperature plot is very noisy. Indeed, as we can see in figure 4b, in our range of relative intensities ($0.5 < I_r/I_b < 0.8$), a small variation in the ratio I_r/I_b means a big change in temperature. In this case, a reduction of noise, without a loss in time resolution (as in Ng *et al.* 1985) can be achieved by spatial averaging over the regions where the shock is flat on both sides of the step, which is possible because such regions are evident in each image.

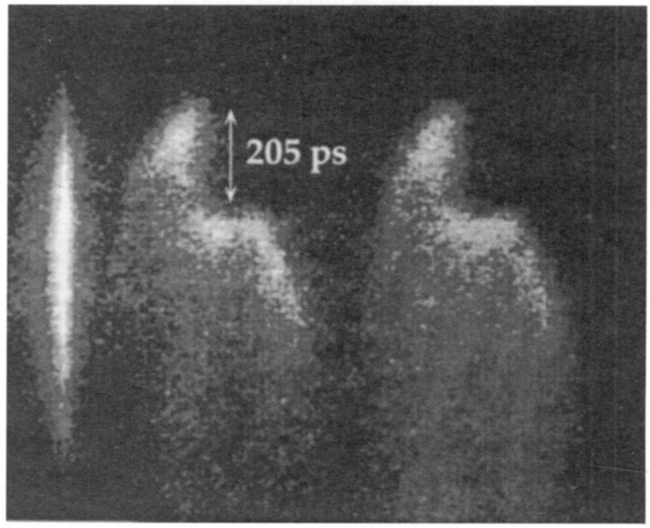

FIGURE 6. Streak camera image obtained with a stepped target (9-μm base + 4.1-μm step) of aluminum. In both emission channels (red to the right and the blue in the center), a temporal difference $\Delta t \approx 205$ ps has been measured between the shock breakthrough times from the base and from the step. The image on the left represents the temporal fiducial.

5. Conclusions and future developments

With the use of an optically smoothed laser beam, we have been able to produce high-quality shock waves with measured velocities of the order of $D \approx 20$ μm/ns, which means a shock temperature $T_s = 3.5$ eV according to SESAME tables. On the other hand, through the "two images" optical diagnostics, we have measured a color temperature $T^* \approx 2$–2.5 eV.

We are currently investigating the causes of such differences and refining the experimental setup. Also, as a future development, three laser beams will be used to increase the total energy on the target. In this way, a wider range of shock pressures will be obtained, allowing a wider range of plasma parameters to be investigated.

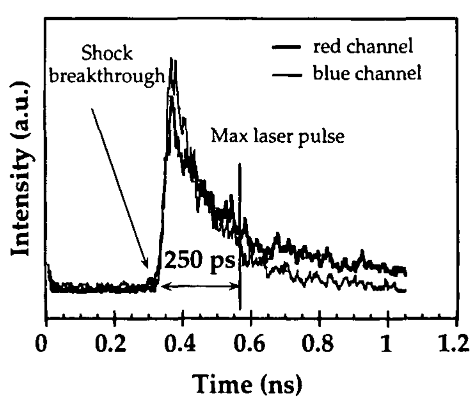

FIGURE 7. Densitometry of both channels of the streak image in figure 6 (signal in arbitrary units as a function of time in ns).

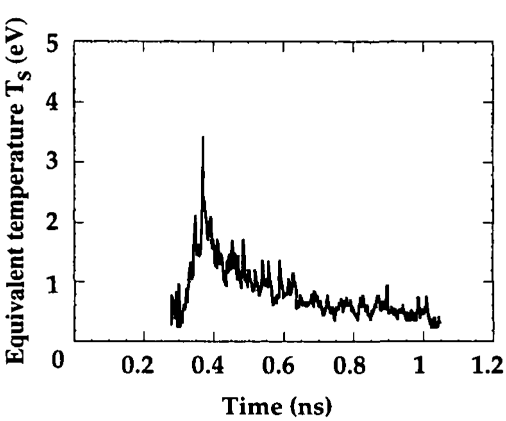

FIGURE 8. Color temperature T^* as a function of time obtained from the ratio between the intensities in the two channels of emission (I_r/I_b).

Acknowledgments

This work has been supported by the "Dense Plasma and Laser Compression Physics" network (EEC contract No. CHRX-CT93-0338) and by the "Access to Large Facilities" (contract No. CHGE-CT-930046) in the framework of the "Human Capital and Mobility" Program.

REFERENCES

BATANI, D. *et al.* 1996 *Laser Part. Beams* **14**, 221.

BENUZZI, A. *et al.* 1996a *Phys. Rev. E* **54**, 2162.

BENUZZI, A. *et al.* 1996b LULI, Ecole Polytechnique Rapport Scientifique 1996.

CAUBLE, R. *et al.* 1993 *Phys. Rev. Lett.* **70**, 2102.

CELLIERS, P. & NG, A. 1993 *Phys. Rev. E* **47**, 3547.

FORTOV, V.E. *et al.* 1992 *Shock Compression of Condensed Matter*, p. 745.

HOLIAN, K.S. 1984 Los Alamos National Laboratory, Report LANL No. LA-10160-MS, UC-34 (unpublished).

HULLER, S. *et al.* 1994 GSI-94 Annual Report.

KOENIG, M. *et al.* 1994 *Phys. Rev. E* **50**, R3314.

LANDSBERG, G.S. 1976 *Optica* (Mir publishers, Moscow).

LÖWER, TH. *et al.* 1994 *Phys. Rev. Lett.* **72**, 3186.

NG, A. *et al.* 1985a *Phys. Fluids* **28**, 2915.

NG, A. *et al.* 1985b *Optics Comm.* **53**, 389.

NUCKOLLS, S.J. *et al.* 1972 *Nature* **239**, 139.

RAGAN, C.E. *et al.* 1982 *Shock Waves in Condensed Matter—1981*, W.J. Nellis, I. Seaman, R.A. Graham, eds. (American Institute of Physics, New York).

SMIRNOV, B.M. 1977 *Introduction to Plasma Physics* (Mir publishers, Moscow).

TRAINOR, R.J. *et al.* 1978 *Phys. Rev. Lett.* **42**, 1154.

ZELDOVICH, YA.B. & RAIZER, YU.P. 1966 *Physics of Shock Waves and High Temperature Hydrodynamic Phenomena* (Academic Press, New York).